

Article citation info:

Smolnicki T, Sokolski P, Strength analysis of welded joints in support structures of heavy machinery subjected to changeable loading conditions, *Eksplatacja i Niezawodność – Maintenance and Reliability* 2024; 26(1) <http://doi.org/10.17531/ein/175889>

Strength analysis of welded joints in support structures of heavy machinery subjected to changeable loading conditions

Indexed by:



Tadeusz Smolnicki^a, Piotr Sokolski^{a,*}

^a Faculty of Mechanical Engineering, Wrocław University of Science and Technology, Poland

Highlights

- The impact of rotation node degradation of BWEs on welded joints' stresses was analysed.
- Models for stress analysis in welded joints bucket wheel excavators were built.
- The applied method is useful for assessing welded joints exposed to variable loads.

Abstract

The durability of bearing units of large machines depends mainly on the condition of their welded joints. With this in mind, we developed numerical models of the analyzed bearing units, for which we performed FEM simulations of the stresses in welded joints in several basic load cases. In each of the respective variants the technical condition of the bearing nodes was different and it corresponded to the severity of the degradation processes. Different positions of the superstructure in relation to the undercarriage were also taken into account. The simulations used the hot-spot method dedicated to FEM analyses of complex welded structures. We discovered that the loads have a significant influence on the values and distribution of von Mises principal stresses and their axial components. Based on the carried out analyses, we identified the most unfavorable load cases that generate the highest stresses in the welded joints of the assessed nodes. We also demonstrated that the applied method effectively assesses the stresses of welded joints subjected to variable working loads.

Keywords

fatigue, welded joint, bucket wheel excavator, finite element method, heavy-duty machine.

This is an open access article under the CC BY license (<https://creativecommons.org/licenses/by/4.0/>)

1. Introduction

Among the most critical challenges in mounting bearings for large machines whose body or working unit rotates around the vertical axis is to ensure that the supporting components have adequate stiffness and strength. The most popular choice is a slewing bearing but the largest machines, such as bucket wheel excavators (BWE), stackers, cranes, etc., also use mechanisms based on conical wheels [39, 40]. The main advantages of the latter solution include the simplicity of its structure and manufacturing technology and lower production cost. One of its disadvantages are high quasi-point loads acting

on the supporting structure, which can lead to high stresses and, consequently, cause fatigue cracks in the welds and the parent material.

Prevention and identification of failures are fundamental in ensuring the reliable operation of BWE. Damages that render a machine nonfunctional generate high costs [35]. For example, 1 hour of downtime of this type of large-scale machine costs over €11,000 [7]. For this reason, ensuring that key BWE nodes, such as rotation mechanisms, remain operational allows for significant financial savings. Both the costs of repairing

(*) Corresponding author.

E-mail addresses:

T. Smolnicki (ORCID: 0000-0003-3917-9952) tadeusz.smolnicki@pwr.edu.pl, P. Sokolski (ORCID: 0000-0003-2407-7988) piotr.sokolski@pwr.edu.pl,

a damaged or broken machine as well as the downtime itself are a significant economic factor. Such negative financial consequences also pertain to many other systems and machinery [37]. For these reasons, great emphasis is placed on reducing financial losses resulting from downtime of large mining machines [16].

Figure 1 shows a diagram of a typical design solution for the rotation node of a large-scale construction machine. Four sets of conical road wheels with multiple rocker arms transmit the resultant vertical force from the body.

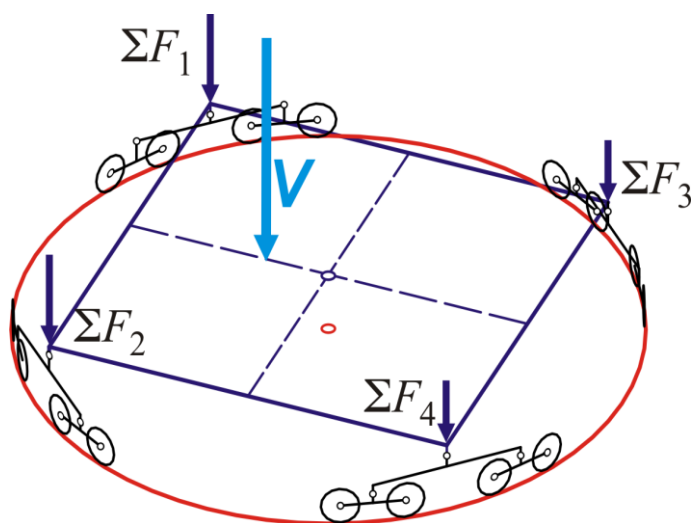


Fig. 1. Diagram of the bearing of a superstructure of a heavy-duty machine machine containing four sets of road wheels with four wheels in each.

Supporting components have the form of complex shell structures joined by welds. The durability of these welded joints has a decisive impact on the correct operation of bearing nodes and, thus, the entire machine. The fatigue lifetime of the entire large-scale construction machine is usually limited by the durability of welded joints [17]. Therefore, this paper evaluates the level of stress of these joints in real working conditions.

Figure 2 shows an example of single set of road wheels and the relevant diagram. The wheels are conical to eliminate slippage on the running rail. Such a system should ensure even loads on the road wheels in a single set but because of friction in the pin joints of the rocker arms the load acting on individual wheels and, consequently, on the supporting components is uneven. The worse the condition of the pins, the greater the differences in the load on respective wheels [41]. Other disadvantages of this type of solution include the lack of a rocker arm between the less loaded sets. As a consequence,

the system is statically indeterminate and the interaction between the wheels and the rail is uneven because the supporting structure of the chassis and the body is deformed. In addition, it was found that the wheels can operate eccentrically.

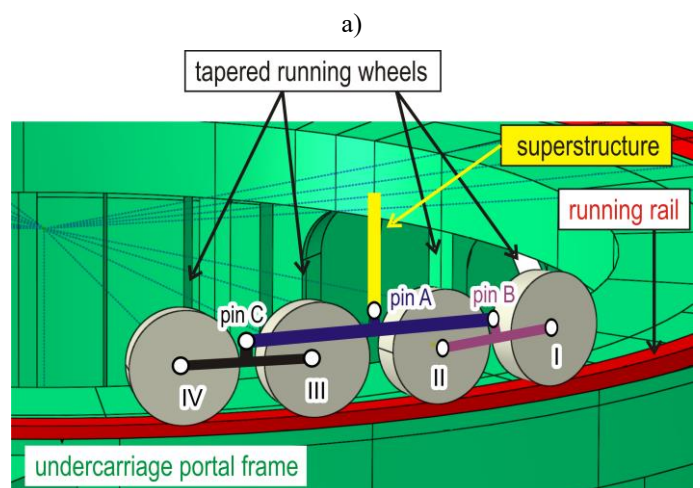


Fig. 2. Example of a technological solution for a single set of road wheels (a) and its diagram (b).

Methods of calculating and evaluating the fatigue life of welded joints

Welded joints are characterized by a high heterogeneity of their structure [14], which results from the need to connect various elements, the use of additional materials and the intensity of thermal processes within such a joint. In order to accurately assess their resistance to fatigue damage, it is necessary to precisely determine the loads and geometrical features of such connections.

The fatigue life of welded structures also depends on factors such as nominal stresses in the analyzed cross-section, stresses at the weld toe, stresses in the notch at the weld location and

stress intensity at the bottom of the crack [18-20, 28, 31, 46].

The International Institute of Welding guidelines can be used for any welded structure, which is particularly useful in cases where there are no normative recommendations and when the applied design solution prevents the use of a given standard [18, 19]. Different calculation methods are used to assess welded joints, including the nominal stress method, the hot-spot stress method, the notch stress method and the fracture mechanics method. These methods involve the use of computer tools based, among others, on FEM [14]. Such an advanced method of computer simulations is a great help in determining the previously mentioned parameters that are necessary to evaluate the analyzed joint. Detailed information on these methods can be found e.g. in [12, 14, 18, 19, 27, 32].

In the hot-spot stress method, the welded joint is assessed without considering the local effect of the notch because the

non-linear increase in stress is introduced by the weld itself. The method consists in surface stress extrapolation at various base points between the outer surface of the sheet (plate) and the edge of the weld or in the linearization of stresses through the sheet (plate) at the edge of the weld. The characteristics and differences between the individual methods are presented in detail in [21]. It should be emphasized that by adopting the hot-spot stress method we can use larger finite elements, extend the concept of effective notch stress to welded aluminum structures and numerically evaluate post-weld heat treatment in the context of fatigue properties [14].

Figure 3 illustrates the hot-spot method, which involves readouts of the stress components at a certain distance from the weld edge and their linear or quadratic extrapolation to the weld edge.

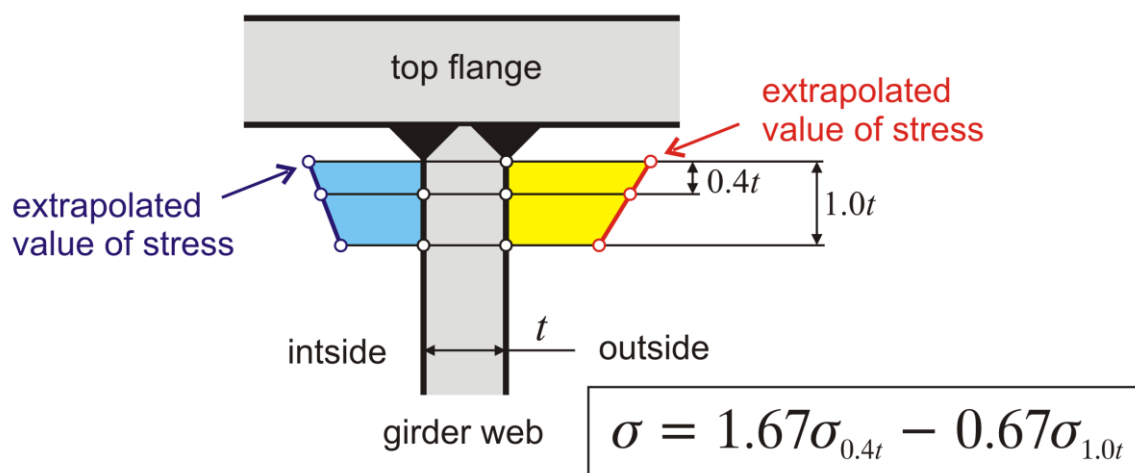


Fig. 3. Extrapolation of stresses to the edge of the weld in the hot-spot method (t – thickness of the sheet).

Many treatments focused on improving the fatigue life of welded joints are local because their effects occur primarily around the weld toe [3]. A critical factor for the durability of welded joints are the residual stresses, which increase the mean stress level in the welded joint [22]. At the same time, the distribution of residual stresses directly impacts the formation of fatigue cracks in welds and is taken into account in the fracture mechanics models [9, 22, 44]. It should be noted that the steel grade does not affect the fatigue strength of steel welded joints [19, 29].

An important novelty in the analysis of welded joints is the replacement of tests of these joints with numerical simulations.

It greatly facilitates the evaluation of these connections. An example of such an approach can be found in [24].

It is worth mentioning that the fatigue life of the analyzed welded joints could be increased through additional technological measures. High frequency mechanical impact (HFMI) is a method that gives outstanding results. It consists of hammering the front surface of the weld with a metal pin (weld toe). This process is performed with a high frequency. As a result, local plastic deformation occurs in the weld and its outer surface is rounded. This outcome makes it possible to reduce the unfavorable effect of the notch and lower stress concentration while creating compressive residual stresses,

which is desirable. In addition, hardness increases in the place where this treatment is applied [2, 15, 29, 34, 45].

Since the HFMI method is also used in the case of welded joints with a certain degree of wear, the remaining durability of welds in the analyzed load-bearing structures can be extended [36].

Other recommended post-welding treatment methods that increase the durability of these joints are peening, grinding and ultrasonic impact treatment [33, 45].

In the case of excessive contact stress values, surface treatment might be necessary to increase the wear resistance of the surface layer [23, 26].

It should be emphasized that numerous activities are carried out to improve the quality of welded joints and their fatigue life. It is equally important to assess the durability of joints that have undergone additional treatment aimed at increasing their durability. Another method worth mentioning is based on assessing the threshold stress intensity after needle peening and is used to improve the durability of butt welds with cracks [13]. There is also a method of determining the relationship between fatigue life and stresses with consideration of selected parameters, such as local deformations. This method was used to evaluate welds whose quality was improved by peening [1, 30]. The last method that is worthy of attention is the application

of the Paris-Erdogan equation after using the HFMI intender. This method makes it possible to obtain a high degree of agreement between the results of the analyses and the experiment [2].

A more detailed overview of the methods for determining the expected life of steel welded joints can be found in [25, 33].

Materials and methods

The object of the study is a KWK-1500s wheeled excavator (Fig. 4), six units of which were produced for operation in Polish open-pit lignite mines. The theoretical capacity of the excavator is 4100 m³/h. It is an excavator with a fixed-length boom. The bridge of the excavator is supported on the chassis. The body turntable 200-mm-wide rail has a radius 6 m, and is supported on the open-section portal frame of the chassis. The wheels are 600 mm in diameter. The height of the ring beam is 4 m. According to the machine documentation, the nominal mining force is 235 kN, and the maximum mining force is 392 kN. According to the machine's stability proof, the body's weight with ballast is 893 Mg, and with the boom horizontally located, the eccentricity of the body load is at a distance of 0.55 m from the axis of rotation in the direction of the counterweight. The body's center of gravity position was verified experimentally before its commissioning.



Fig. 4. View of the KWK-1500s excavator.

We focused our research on the rotation node in one of the KWK-1500s wheeled excavators, with the resultant load from the body equal to about 9.5 MN. The machine uses bogies. The

ring girder of the chassis has an open structure similar to an open channel. Figure 5 shows the angle of the body position relative to the chassis. The zero angle was assumed for the body

positioned perpendicular to the plane of symmetry of the chassis.

The support structure of the excavator is made of S355 steel, which provides good weldability and stable high-strength properties. At the same time, this material is relatively inexpensive. On the other hand, the rails of the excavator are made of C55 steel. During the modelling of the object, all elements were given appropriate parameters.

After 20 years of the machine's operation, the load-bearing structure of its chassis suffered significant degradation and the welded connection between the 40 mm thick flange and the 25 mm thick web located under the running rail was destroyed. An incomplete butt weld had been used for the connection and about 50% of the total circumferential length of the weld was damaged. Damage locations are shown in Figure 6.

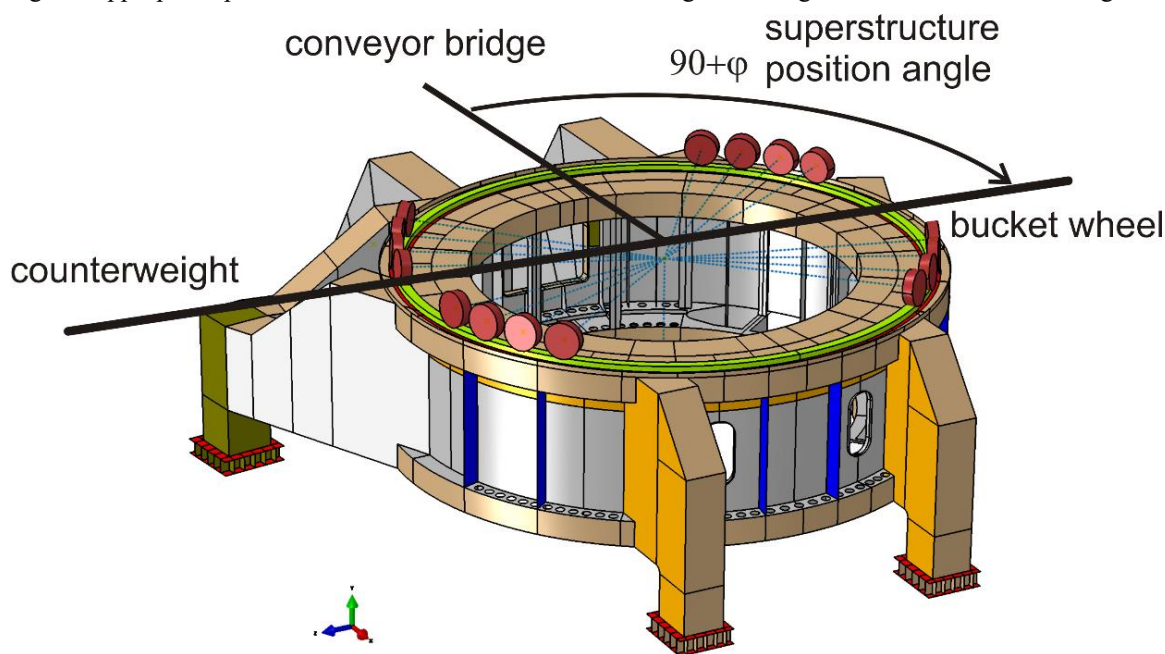


Fig. 5. Chassis model of a large excavator with a running rail and wheels.

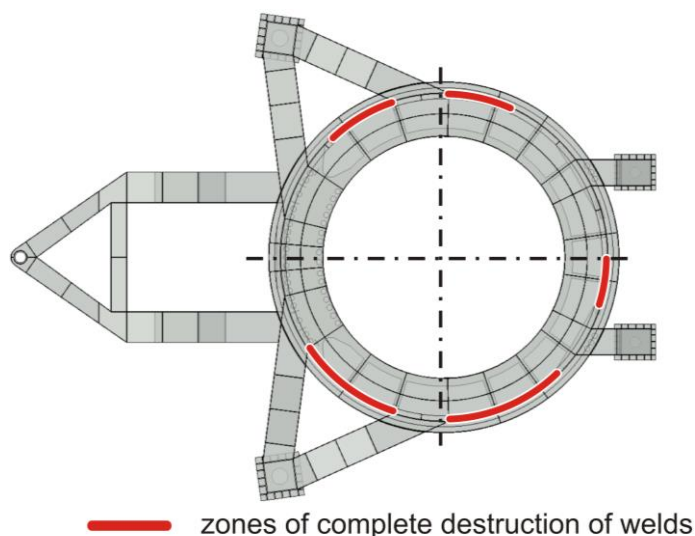


Fig. 6. Zones of complete failure of the weld between the flange and the web under the running rail. Location of zones marked according to [38].

We used flaw detection tests to assess the technical condition of welded joints. By carrying out experiments we verified the weight and location of the body's center of gravity. Additionally,

we measured the deformations caused by road wheels in the web of the ring girder. These measurements showed wheel overload due to pin locking (Fig. 2b): 32.5% due to pin A locking and 33.7% due to pin B or pin C locking. We decided to carry out an advanced FEM analysis of the level of stress in welds. The nominal stress method, the hot-spot method or the effective notch stress method [4, 5, 8, 12, 18-20, 42, 43, , 47] are most often used to assess stresses in welds subjected to variable loads.

However, typical strength models built during the design of superstructures turned out to be unusable due to too low discretization density and model size. The minimum size of finite elements in such models is two or three sheet thicknesses, which in the analyzed case is approximately 50 mm. The size of the machine also makes it impossible to discretize by volume elements. The only alternative is the hot-spot method developed by Hobbacher and the application of the shell model. We used a 4-node thick shell finite element from the ABAQUS library to build the gantry frame model. The rail was modeled with hexahedral elements, and the wheels as discrete rigids (Fig. 7).

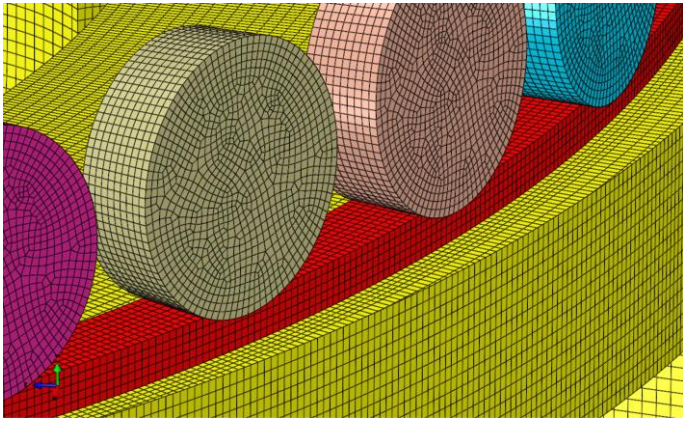


Fig. 7. Discretization of the system: undercarriage gantry frame - running rail - running wheels (fragment).

The computational models used in constructing the KWK-1500s excavators were highly simplified and did not consider local phenomena since the ring girder was treated as a curved beam. Later FEM models used for numerical analyses after weld cracking between the top flange of the girder and the web were shell models. However, the size of the finite elements did not allow an accurate analysis of the phenomena occurring in those joints.

FEM does not allow reading the stress values directly in the welded joint. The International Institute of Welding recommends the stress extrapolation method proposed by Hobbacher. However, the problem occurs while applying this method to such large structures as bucket wheel excavators. It is necessary to find out the stress values at well-defined points at a small distance from the weld edge. The models built are characterized by very small finite element discretization. It also became necessary to carry out calculations for many different positions of the body relative to the chassis (every half wheelbase of the running wheel). It is also needed to consider the contact between the running rail and the girder flange, and between the running wheels and the rail. Such detailed analyses of comparable large objects considering local phenomena are

lacking in the literature.

During the operation of the machine, both the value of the resultant vertical load from the body and its position change. DIN 22261 [48] gives the combinations of loads for strength calculations. In the case of operational strength, the weight of the body, the peripheral and lateral forces of mining, the weight of debris and excavated material, the longitudinal ground inclination and transverse ground inclination, and the dynamic excesses are adopted for the calculations. At the nominal mining force, the eccentricity of the axial load is 0.97 m, and at the maximum, it increases to a value of 1.64 m. The maximum eccentricity is at the horizontal position of the bucket wheel boom. In the case of the analyzed machine, measurements were also carried out to determine the forces in the ropes of the draw-wheel system during mining [6, 10, 11]. Based on the measurements and the proof of the machine's stability, it was found that during mining, the machine is overloaded, and the value of the peripheral excavating force is higher than that stated in the machine's documentation and reaches a value of about 330 kN. In such a case, the load distribution for wheel sets is 68% on the side of the bucket wheel to 32% under the counterweight. That corresponds to an eccentricity of 1.4 m. Such a distribution of loads was assumed in the simulations.

Due to the distance of the rotation node from the bucket wheel, mining dynamics have less influence on the fatigue of the weld under the running rail than the rolling of successive running wheels.

Due to the different possible conditions of the rocker arm pins, three loading scenarios were assumed: fully operational rocker arms (no friction), pin A locked, and pin B locked (Fig. 8). Based on the tests carried out on the physical object, the eccentricity of the wheels was assumed to be equal to 0.5 of the width of the running rail.

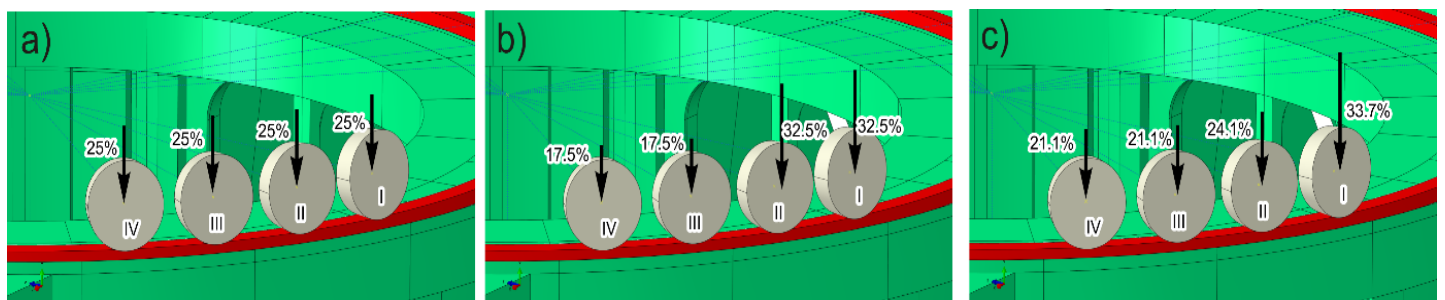


Fig. 8. Different loading scenarios for the wheel in the set: a) pins in working order, b) pin A locked, c) pin B locked.

Results and discussion

We calculated different positions of the superstructure in relation to the undercarriage with an increment equal to the wheelbase of the road wheels. Geometrical nonlinearity is included. We chose the most representative results for the selected locations.

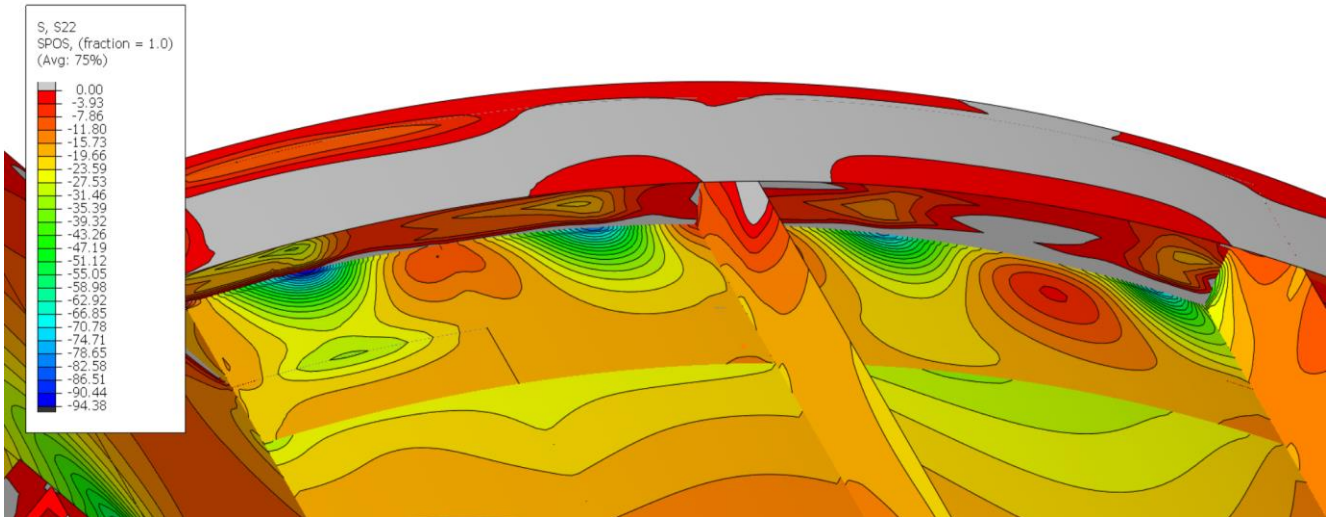


Fig. 9. Stress in the axial direction on the outer wall of the web, superstructure position 64° , fully operational pins (markings limited to a negative stress range) in [MPa].

Figure 10 shows the stresses σ_Y on both sides of the web shell when the body is rotated relative to the chassis by 32° . The areas of operation of the successive road wheels have been marked. The force the wheels exerts propagates in the girder shell similarly to the Flamant solution [41]. Differences from the Boussinesq equation result from the curvature of the shell, changes in sheet thickness and the presence of supports, ribs and webs. For this reason, despite equal forces, the effort under each wheel is different. There is compression at the edge of the weld directly below the wheels and tension between the wheels. This means that the rolling of the wheels causes a cyclic change in the stress sign. When the body is in the abovementioned position, the point under wheel I, located away from any reinforcements, is the most sensitive, whereas the point under wheel IV, located at the far end of the support arm, is the least sensitive. Von Mises stresses for the same conditions are shown in Figure 11. What is noticeable are lower values of von Mises stresses than the value of the axial component σ_Y and a different character of the stress distribution on both sides of the web. This is due to the eccentric influence of the wheel on the rail and the curvature of the web.

Figure 9 shows the stress in the flange in the axial direction σ_Y , i.e. in the direction of the load from the wheels, when all pins are operational, with the body rotated by the angle φ 64° relative to the chassis. The angle is defined in Figure 5. For ease of reading, subsequent results are limited to the web of the annular girder only at a short distance from the weld.

For the same body position, calculations were made with pin A locked. According to the strain gauge measurements, in this case, every first and second wheel in each set is loaded with a force equal to 32.5% of the total load, as shown in the diagram in Figure 8b. The results are shown in Figures 12 and 13. There was a significant increase of 19% in stress values. A similar increase was observed with pin B locked. Extreme values are listed in Table 1.

Table. 1. Summary of extreme stress values with operable and locked pins in MPa.

	von Mises stress σ_{HM}	min axial stress σ_{Ymin}	max axial stress σ_{Ymax}	stress range $\Delta\sigma$
operable pins	86.2	-99.1	16.6	115.5
locked pin A	102.4	-117.6	17.6	135.2
locked pin B	100.7	-115.3	16.9	132.2

The determined stress values do not take into account the hot-spot method. The stress values in the FEM mesh nodes in the web-flange connection are averaged. A linear extrapolation was performed. The results from the weld edge are presented as stress curves along the circumferential path, i.e., along the weld, and axial (vertical) path under each trolley wheel (Fig. 14).

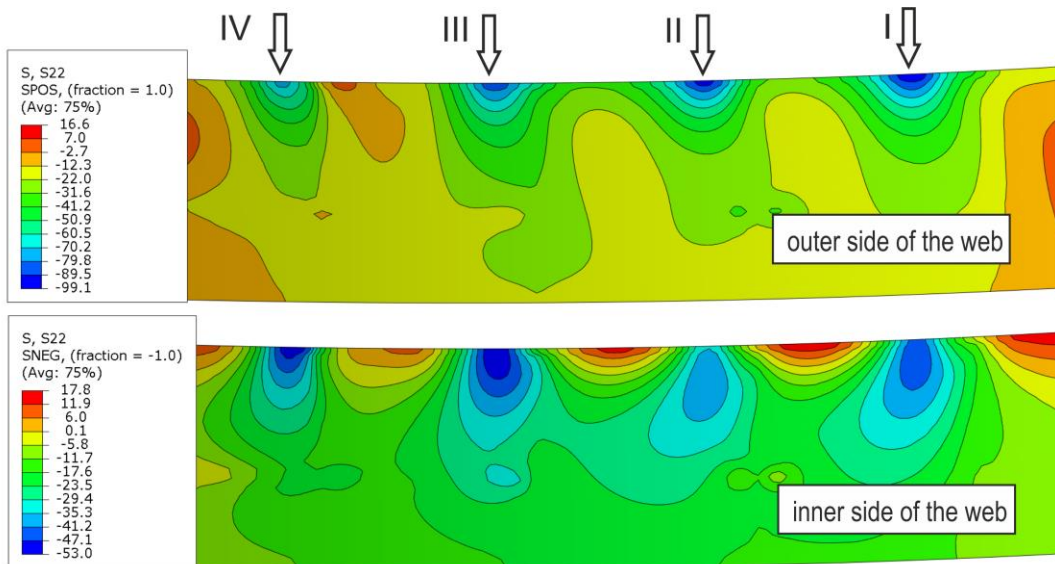


Fig. 10. Stress in the axial direction σ_Y on the outer and inner wall of the web, superstructure position 32°, operable pins in [MPa].

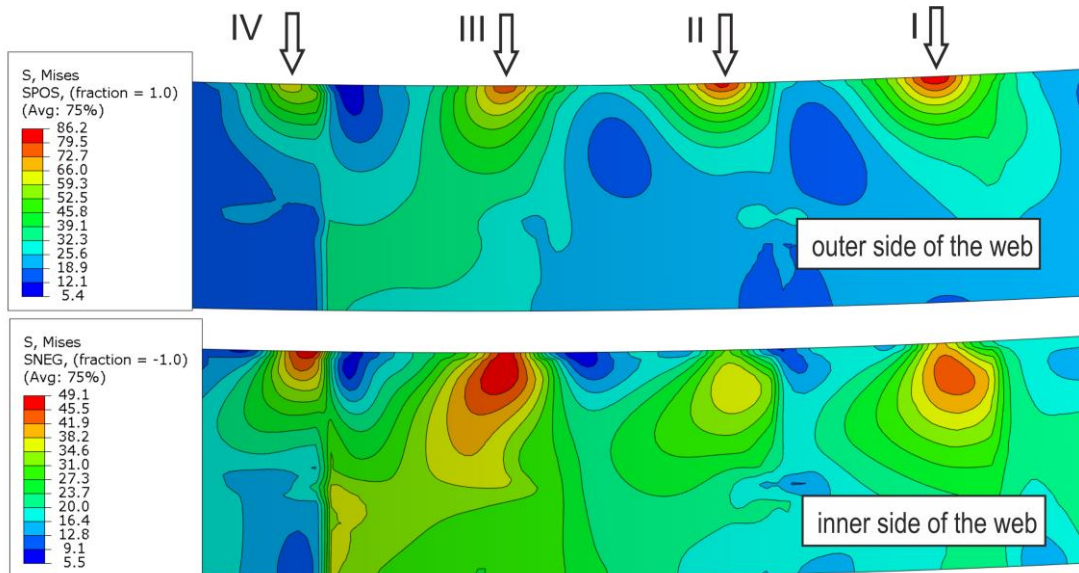


Fig. 11. Von Mises stress on the outer and inner wall of the web, superstructure position 32°, operable pins, in [MPa].

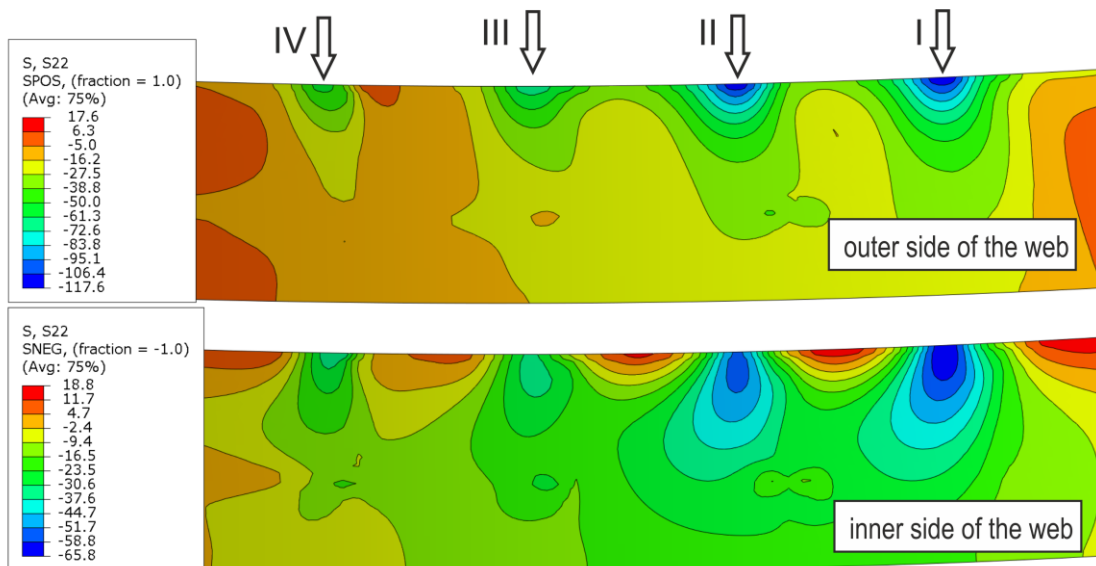


Fig. 12. Stress in the axial direction on the outer and inner wall of the web, superstructure position 32°, locked pin A in [MPa].

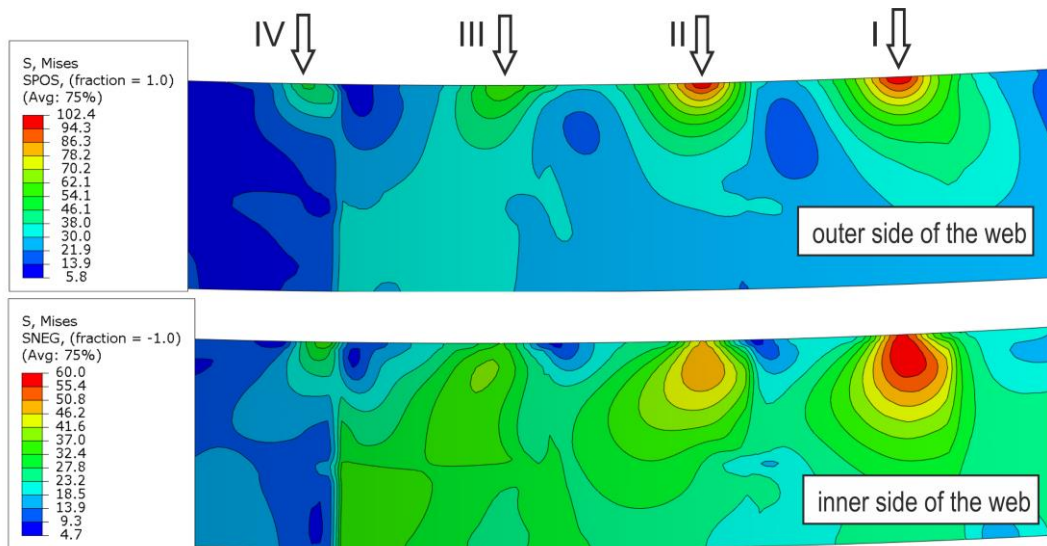


Fig. 13. Von Mises stress on the outer and inner wall of the web, superstructure position 32°, locked pin A in [MPa].

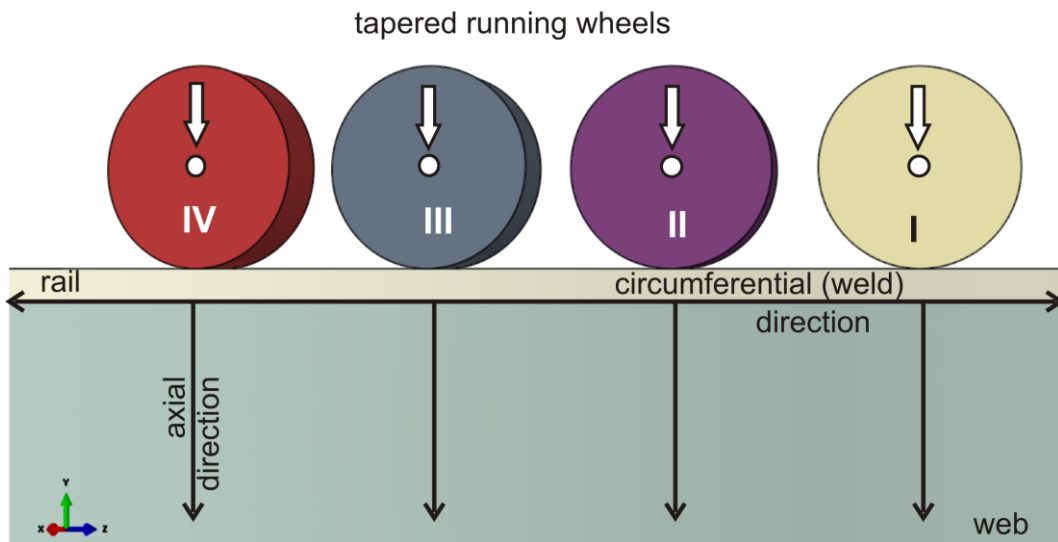
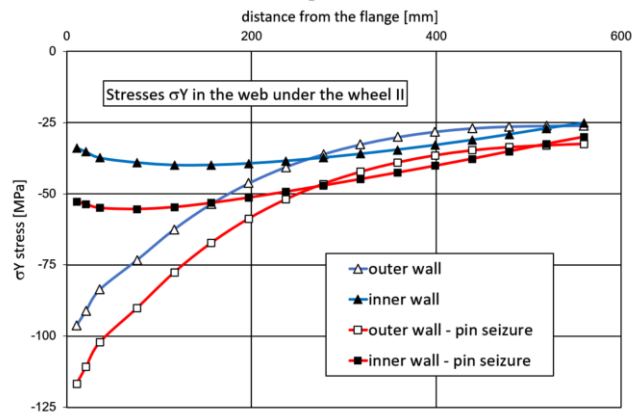
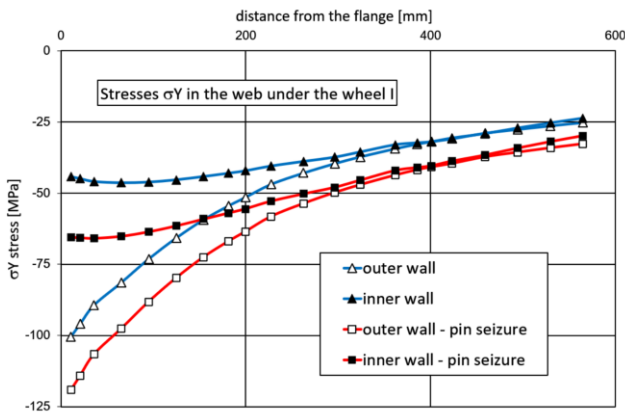


Fig. 14: Schematic of the paths on which the stress values were read along the web in the axial and circumferential directions.

Figure 15 presents the course of stresses on the paths along the web for the body positioned at an angle of 32°. The curves at the functional pins are marked in blue, and the curves at the locked pin A in red. The last value of the curve at the weld edge was determined by interpolation. When the pin is locked, there

is an increase in the level of stress under each wheel. The course of stresses is different on the outer wall where the stress increases parabolically as it approaches the weld, than on the inner wall, where the extreme value is several dozen millimeters away from the weld.



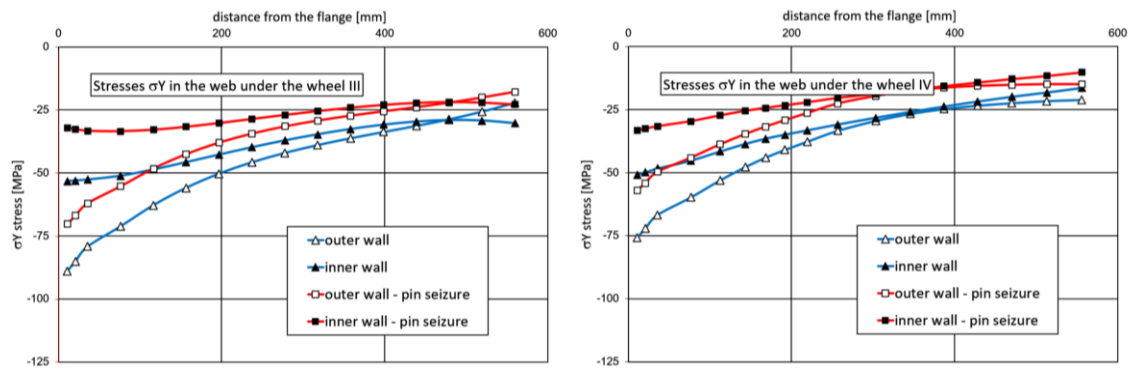


Fig. 15. Stresses in the axial direction on the path along the web under wheels I - IV on the outside (unfilled markers) and inside (filled markers) of the web with the pins functional (triangular markers) and the pin A blocked (square markers).

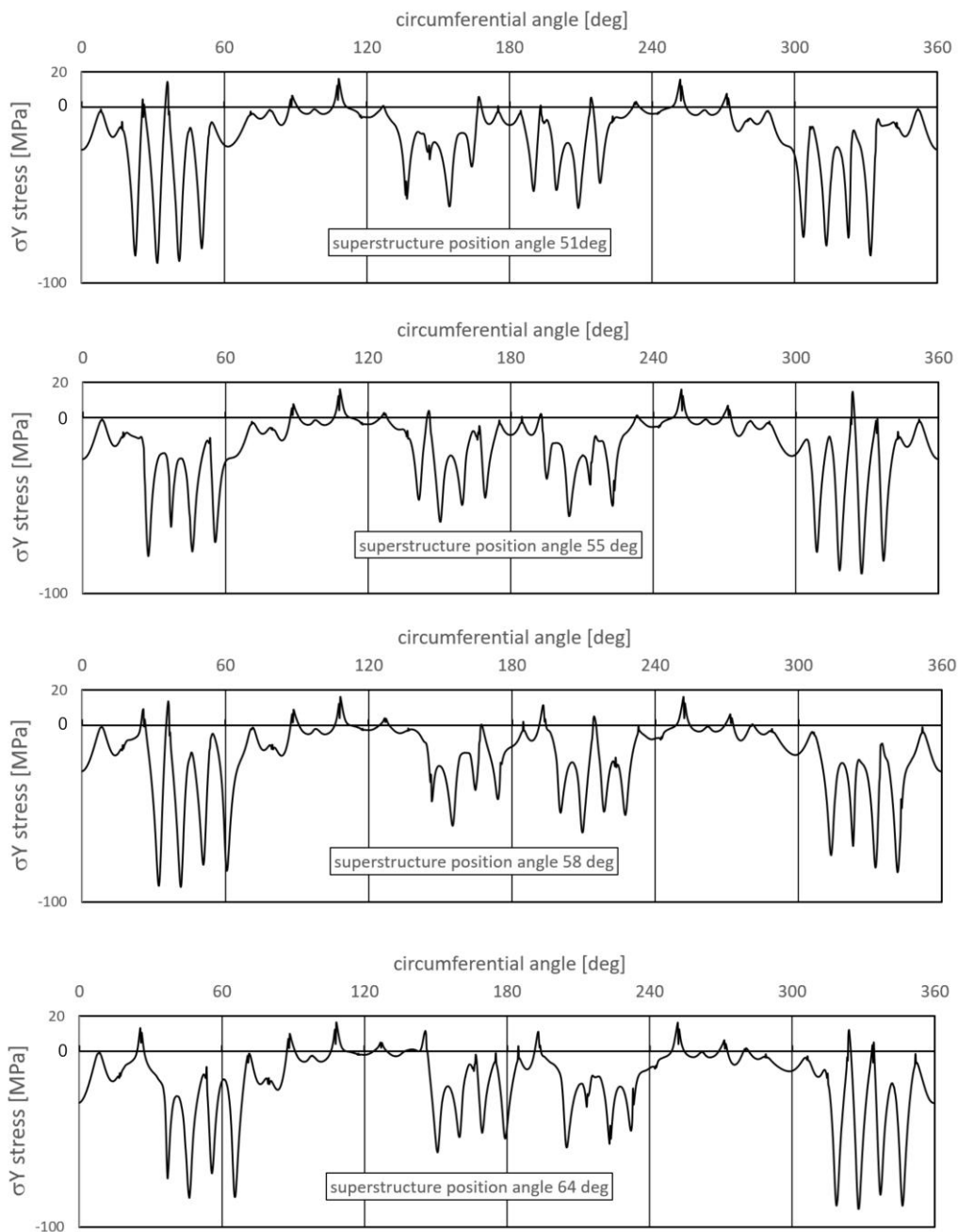


Fig. 16. Stress hot-spots in the axial direction at the weld edge on the outer side determined by the hot-spot method for four different superstructure positions (51°, 55°, 58°, 64°).

The course of stress along the perimeter of the weld was analyzed for various body positions in relation to the chassis. Figure 16 shows the waveforms for the angles φ equal to 51° , 55° , 58° and 64° and for fully functional pins. In this angular range, strain gauge measurements revealed that the differences in the impact of particular wheels were the most significant due to the locking of the pins. Depending on the position, there are clear differences in the weld effort under the individual wheels of the bogie. Extreme values are obtained when the wheel is

located between the diaphragms and the ribs relieving the web. Figure 17 shows the course of the stress for the angle φ equal to 64° with marked extremes related to the successive wheels. In order to validate the values of the courses with locked pins, the calculations for these operating cases were repeated. Figure 18 shows a graph with results limited to the interaction of circles I - IV. The graph shows extreme values in boxes. It was found that when the bogie with damaged rocker arms is traveling, the stress range $\Delta\sigma$ exceeds the value of 135 MPa.

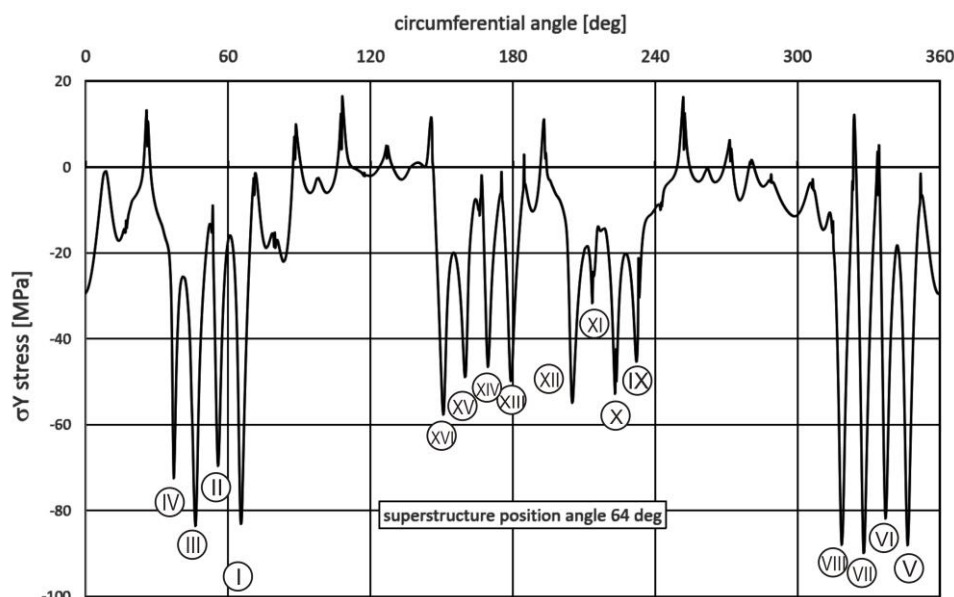


Fig. 17. Stresses in the axial direction at the weld edge on the outer side determined by the hot-spot method at superstructure position 64° , marked wheels.

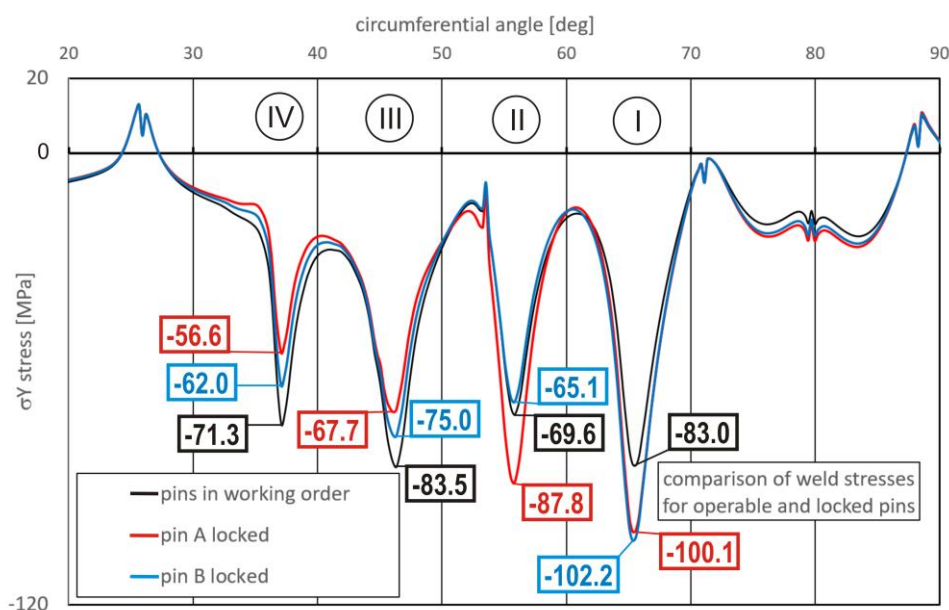


Fig. 18. Stresses in the axial direction at the edge of the weld from the outside determined by the hot-spot method at superstructure position 64° in the area of wheels I-IV, with fully functional pins (black), locked pin A (red), locked pin B (blue). Extreme values are given.

Before commissioning the machine, strain gauge measurements of the chassis superstructure's strain when rotating without mining were carried out [6, 10, 11]. We used those results for the validation of our model. Figure 19 shows the maximum values of von Mises stresses in six sections of the

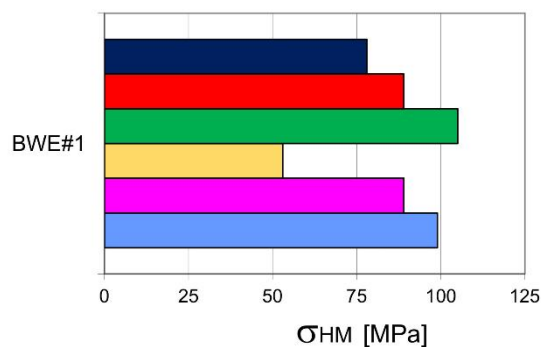
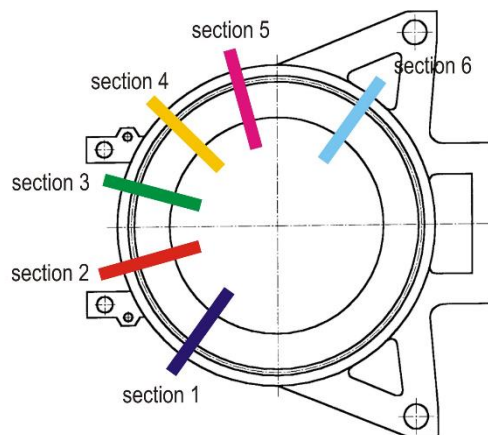


Fig. 19. Von Mises stresses in different sections of the excavator (based on [6, 10, 11]).

Conclusions

Using the portal frame of an excavator chassis as an example, we have shown the impact of road wheels on the load-bearing structure of the chassis, and in particular on the effort of the weld between the web and the upper flange of the ring girder. The analysis revealed significant fatigue damage to these welds. The performed strain gauge measurements [41] showed deteriorated pin connections and uneven loads of the road wheels, and the observations of the interaction between the wheels and the rails showed an eccentric impact of the wheels on the rail.

Due to the size of this type of machinery, the only computational model that can be used is a shell model with dense discretization and distribution of FEM mesh nodes in accordance with the hot-spot method. Calculations were carried out for different body positions in relation to the chassis and different operating conditions of the bogie rocker pins. The hot-spot method was used to determine stresses on the weld edge inside and outside the girder and the results are presented for selected body positions relative to the chassis.

Depending on the position of the body, there were differences in the sensitivity of the weld to the impact of the wheel. The impact was the highest when the wheel was located between the diaphragms of the ring girder. Below the wheel, the weld is compressed, but halfway between the wheels it is

excavator. Low values of von Mises stresses were obtained. However, the stresses were not determined directly in the weld but at selected cross-section points distant from the weld.

subject to tension. Subsequently, the sign of the stress changes, which considerably increases the value of the stress range. For this reason, the usual von Mises stresses are unsuitable for stress analysis of the weld. When performing calculations, the assumed position of the body in relation to the chassis should ensure that the wheels are between the diaphragms. It is also necessary to check the different positions of the body relative to the chassis. The best course of action would be to analyze all possible body positions within the operational range at angle increments equal to half the wheelbase. However, that would produce several dozen load cases requiring significant computational time and an automated generation of individual models, as well as extraction and analysis of results. For a researcher experienced in analyzing this type of load-bearing structures it is sufficient to select the worst positions, particularly when the places of weld damage are known, as in the analyzed example.

We found that, unlike slewing bearings which act “smoothly” on the load-carrying structures of machines, the same interaction in the case of bogies with wheels, despite the use of massive rails, causes many defects in the load-carrying structure, especially in the weld located under the rail, whereas the considerable distance between the wheels changes the sign of stress.

The condition of the load-carrying structure is also influenced by the locking of the rocker arm pins. In the analyzed

example, an increase in the wheel load by 30% due to pin lock causes an increase in stress in the weld by about 20% and a similar increase in the range of stresses. With locked rocker arms, the maximum value of the stress range, i.e. the difference between the maximum and minimum stress value in the weld, was as high as 135 MPa. According to the guidelines for constructing welded joints, this value should not exceed 100 MPa. It should be noted that von Mises stresses did not exceed 100 MPa at the connection of the web and flange.

The presented results show that this type of procedure is useful in analyzing the effort of welded joints subjected to

variable loads from road wheels. However, this method requires an accurate discretization under the requirements of the hot-spot method, a regular mesh of finite elements, a good knowledge of modeling in the field of geometric nonlinearity, and an outstanding ability to analyze the results.

One should be aware that FEM is an approximate method due to simplifications in modeling, interpolation in finite elements and the adoption of boundary conditions and load associations. However, due to our model's details in the analyzed area, it is much more accurate than those used so far and enables us to demonstrate the cause of cracks.

References

1. Al-Karawi H, von Bock und Polach RUF, Al-Emrani M. Fatigue crack repair in welded structures via tungsten inert gas remelting and high frequency mechanical impact. *J Constr Steel Res.* 2020 Sep 1;172, <https://doi.org/10.1016/j.jcsr.2020.106200>.
2. Al-Karawi H, von Bock und Polach RUF, Al-Emrani M. Fatigue life extension of existing welded structures via high frequency mechanical impact (HFMI) treatment. *Eng Struct.* 2021 Jul 15;239, <https://doi.org/10.1016/j.engstruct.2021.112234>.
3. Al-Karawi HA. Fatigue life estimation of welded structures enhanced by combined thermo-mechanical treatment methods. *J Constr Steel Res.* 2021 Dec 1;187, <https://doi.org/10.1016/j.jcsr.2021.106961>.
4. Al Zamzami I, Susmel L. On the accuracy of nominal, structural, and local stress based approaches in designing aluminium welded joints against fatigue. *Int J Fatigue.* 2017 Aug 1;101:137–58, <https://doi.org/10.1016/j.ijfatigue.2016.11.002>.
5. Amarir I, Mounir H, Marjani A El. Effect of Temperature and Thickness of the Weld Bead on the Durability of Welded Rectangular Profiles under Damped Loads for Electrical Vehicles Utilization. 2018 6th International Renewable and Sustainable Energy Conference (IRSEC), Rabat, Morocco, 2018, pp. 1-6, <https://doi.org/10.1109/IRSEC.2018.8702834>.
6. Babiarz S, Dudek, D. Chronicle of failures and catastrophes of basic machinery in the Polish open-pit mining industry. Wrocław University of Science Publishing House: Wrocław, Poland, 2007. (In Polish).
7. Bošnjak S, Pantelić M, Zrnić N, Gnjatović N, Dordević M. Failure analysis and reconstruction design of the slewing platform mantle of the bucket wheel excavator O&K SchRs 630. *Eng Fail Anal.* 2011 Mar;18(2):658–69, <https://doi.org/10.1016/j.engfailanal.2010.09.035>.
8. Cheng B, Abdelbaset H, Tian L, Li HT, Su Q. Hot spot stress investigation on rib-to-deck-to-floor beam connections in UHPC reinforced OSDs. *J Constr Steel Res.* 2021 Apr 1;179, <https://doi.org/10.1016/j.jcsr.2020.106517>.
9. Cui C, Zhang Q, Bao Y, Bu Y, Luo Y. Fatigue life evaluation of welded joints in steel bridge considering residual stress. *J Constr Steel Res.* 2019 Feb 1;153:509–18, <https://doi.org/10.1016/j.jcsr.2018.11.003>.
10. Dudek D, Kanczewski P, Sokolski M. Experimental analysis of ring girder fatigue of a bucket wheel excavator. In: Development of fundamentals of construction, operation and testing of heavy working machinery - including construction machinery. I Conference of the Central Basic Research Program, Part 1. Scientific Papers of the Institute of Construction and Operation of Machinery of Wrocław University of Science. Conferences; No. 13, pp. 97-105, Wrocław, 1987. (In Polish).
11. Dudek D, Rusiński E, Sokolski M, Włodarczyk J. Stress analysis of ring girder of steel structure of KWK 1500s chassis on the basis of strain gauge measurements of stress course and local displacements: Part II. Performance testing of the ring girder KWK 1500s. Reports of the Institute of Construction and Operation of Machinery of Wrocław University of Science. SPR No. 57, Wrocław, 1985. (In Polish).
12. Feng L, Qian X. A hot-spot energy indicator for welded plate connections under cyclic axial loading and bending. *Eng Struct.* 2017 Sep 15;147:598–612, <https://doi.org/10.1016/j.engstruct.2017.06.021>.
13. Fueki R, Takahashi K. Prediction of fatigue limit improvement in needle peened welded joints containing crack-like defects. *International Journal of Structural Integrity.* 2018;9(1):50–64, <https://doi.org/10.1108/IJSI-03-2017-0019>.
14. Fuštar B, Lukačević I, Dujmović D. Review of Fatigue Assessment Methods for Welded Steel Structures. Vol. 2018, *Advances in Civil Engineering.* Hindawi Limited; 2018, <https://doi.org/10.1155/2018/3597356>.

15. Fuštar B, Lukačević I, Skejić D, Lukić M. Two-stage model for fatigue life assessment of high frequency mechanical impact (HFMI) treated welded steel details. *Metals (Basel)*. 2021 Aug 1;11(8), <https://doi.org/10.3390/met11081318>.
16. Gnjatović N, Bošnjak S, Stefanović A. Analysis of the Dynamic Response as a Basis for the Efficient Protection of Large Structure Health Using Controllable Frequency-Controlled Drives. *Mathematics*. 2023 Jan 1;11(1), <https://doi.org/10.3390/math11010154>.
17. Grabowski P, Jankowiak A, Marowski W. Fatigue lifetime correction of structural joints of opencast mining machinery. *Eksploatacja i Niezawodność - Maintenance and Reliability* 2021; 23 (3): 530–539, <https://doi.org/10.17531/ein.2021.3.14>.
18. Hobbacher AF. The new IIW recommendations for fatigue assessment of welded joints and components - A comprehensive code recently updated. *Int J Fatigue*. 2009 Jan;31(1):50–8, <https://doi.org/10.1016/j.ijfatigue.2008.04.002>.
19. Hobbacher AF. New developments at the recent update of the IIW recommendations for fatigue of welded joints and components. *Steel Construction*. 2010 Dec;3(4):231–42, <https://doi.org/10.1002/stco.201010030>.
20. Hobbacher AF. IIW Collection Recommendations for Fatigue Design of Welded Joints and Components [Internet]. Berlin: Springer International Publishing; 2015. Available from: <http://www.springer.com/series/13906>, <https://doi.org/10.1007/978-3-319-23757-2>
21. Iqbal N, Fang H, Naseem A, Kashif M, De Backer H. A numerical evaluation of structural hot-spot stress methods in rib-to-deck joint of orthotropic steel deck. *Applied Sciences (Switzerland)*. 2020 Oct 1;10(19):1–19, <https://doi.org/10.3390/app10196924>.
22. Jiang W, Xie X, Wang T, Zhang X, Tu ST, Wang J, Zhao X. Fatigue life prediction of 316L stainless steel weld joint including the role of residual stress and its evolution: Experimental and modelling. *Int J Fatigue*. 2021 Feb 1;143, <https://doi.org/10.1016/j.ijfatigue.2020.105997>.
23. Kombayev K, Muzdybayev M, Muzdybayeva A, Myrzabekova D, Wieleba W, Leśniewski T. Functional Surface Layer Strengthening and Wear Resistance Increasing of a Low Carbon Steel by Electrolytic-Plasma Processing. *Strojnicki Vestnik - Journal of Mechanical Engineering*. 2022;68(9):542–51, <https://doi.org/10.5545/sv-jme.2022.147>.
24. Królicka A, Radwański K, Kuziak R, Zygmunt T, Ambroziak A. Microstructure-based approach to the evaluation of welded joints of bainitic rails designed for high-speed railways. *J Constr Steel Res*. 2020 Dec 1;175, <https://doi.org/10.1016/j.jcsr.2020.106372>.
25. Kumar H, Thakur M, Raj J, Baghel A. A Review on Fatigue Life Estimation of Welded Joints. *IJSTE [Internet]*. 2018;Volume 4(Issue 7):24–31. Available: www.ijste.org
26. Lachowicz MM, Leśniewski T, Lachowicz MB. Effect of Dual-stage Ageing and RRA Treatment on the Three-body Abrasive Wear of the AW7075 Alloy. *Strojnicki Vestnik - Journal of Mechanical Engineering*. 2022;68(7–8):493–505, <https://doi.org/10.5545/sv-jme.2022.142>.
27. Łagoda T, Głowačka K. Fatigue life prediction of welded joints from nominal system to fracture mechanics. *Int J Fatigue*. 2020 Aug 1;137, <https://doi.org/10.1016/j.ijfatigue.2020.105647>.
28. Lee JM, Seo JK, Kim MH, Shin SB, Han MS, Park JS, Mahendran M. Comparison of hot spot stress evaluation methods for welded structures. *International Journal of Naval Architecture and Ocean Engineering*. 2010 Dec;2(4):200–10, <https://doi.org/10.2478/IJNAOE-2013-0037>.
29. Leitner M, Simunek D, Shah SF, Stoschka M. Numerical fatigue assessment of welded and HFMI-treated joints by notch stress/strain and fracture mechanical approaches. *Advances in Engineering Software*. 2016 Jan 1;120:96–106, <https://doi.org/10.1016/j.advengsoft.2016.01.022>.
30. Lihavainen VM, Marquis G. Fatigue life estimation of ultrasonic impact treated welds using a local strain approach. *Steel Res Int*. 2006;77(12):896–900, <https://doi.org/10.1002/srin.200606478>.
31. Liu R, Ji B, Wang M, Chen C, Maeno H. Numerical Evaluation of Toe-Deck Fatigue in Orthotropic Steel Bridge Deck. *Journal of Performance of Constructed Facilities*. 2015 Dec;29(6), [https://doi.org/10.1061/\(ASCE\)CF.1943-5509.0000677](https://doi.org/10.1061/(ASCE)CF.1943-5509.0000677).
32. Liu S, Liu Y. Summary of research on fatigue life assessment of welded joints. *J. Phys.: Conf. Ser.* 1303 012002 2019, <https://doi.org/10.1088/1742-6596/1303/1/012002>
33. Manai A. A framework to assess and repair pre-fatigued welded steel structures by TIG dressing. *Eng Fail Anal*. 2020 Dec 1;118, <https://doi.org/10.1016/j.engfailanal.2020.104923>.
34. Mikkola E, Remes H, Marquis G. A finite element study on residual stress stability and fatigue damage in high-frequency mechanical impact (HFMI)-treated welded joint. *Int J Fatigue*. 2017 Jan 1;94:16–29, <https://doi.org/10.1016/j.ijfatigue.2016.09.009>.
35. Milenović I, Bošnjak S, Gnjatović N, Obradović A. Bucket wheel excavators with a kinematic breakdown system: Identification and

- monitoring of the basic parameters of static stability of the slewing superstructure. *Eksploatacja i Niezawodność - Maintenance and Reliability* 2022; 24(2), <https://doi.org/10.17531/ein.2022.2.17>.
36. Nazzal SS, Mikkola E, Yıldırım HC. Fatigue damage of welded high-strength steel details improved by post-weld treatment subjected to critical cyclic loading conditions. *Eng Struct.* 2021 Jun 15;237, <https://doi.org/10.1016/j.engstruct.2021.111928>.
 37. Niewczas A, Móravski Ł, Rymarz J, Dębicka E, Hołyszko P. Operational risk assessment model for city buses. *Eksploatacja i Niezawodność - Maintenance and Reliability* 2023; 25(1), <https://doi.org/10.17531/ein.2023.1.14>.
 38. Rosik R. Methodology of evaluation of degradation processes of rail nodes of rotation of bodies of working machines. [Wrocław]: (PhD Thesis), Wrocław University of Science; 2007 (in Polish).
 39. Smolnicki T. Physical Aspects of the Coherence Between the Large-Size Rolling Bearings and Deformable Support Structures. Wrocław University of Technology Publishing House. Wrocław, Poland, 2002. (In Polish).
 40. Smolnicki T. Large-Size Slewing Joints: Global and Local Issues. Wrocław University of Technology Publishing House: Wrocław, Poland, 2013. (In Polish).
 41. Sokolski P, Smolnicki T. A method for monitoring the technical condition of large-scale bearing nodes in the bodies of machines operating for extended periods of time. *Energies* 2021; 14 (19): article number 6637, <https://doi.org/10.3390/en14206637>.
 42. Szala G, Ligaj B. Analysis of a Simplified Method for Determining Fatigue Charts $\Delta s-N$ on the Example of Welded and Soldered Connectors. *Polish Maritime Research.* 2018 Jun 1;25(2):92–9, <https://doi.org/10.2478/pomr-2018-0059>.
 43. Śledziwski K. Fatigue assessment for selected connections of structural steel bridge components using the finite elements method. In: *AIP Conference Proceedings.* American Institute of Physics Inc.; 2018, <https://doi.org/10.1063/1.5019154>.
 44. Taheri S, Fatemi A. Fatigue crack behavior in power plant residual heat removal system piping including weld residual stress effects. *Int J Fatigue.* 2017 Aug 1;101:244–52, <https://doi.org/10.1016/j.ijfatigue.2016.11.004>.
 45. Tang L, Ince A, Zheng J. Numerical modeling of residual stresses and fatigue damage assessment of ultrasonic impact treated 304L stainless steel welded joints. *Eng Fail Anal.* 2020 Jan 1;108, <https://doi.org/10.1016/j.engfailanal.2019.104277>.
 46. Vantadori S, Giordani F, Fortese G, Iturrioz I. Hot-spot localisation according to the critical plane-based approach. *Int J Fatigue.* 2018 Nov 1;116:669–76, <https://doi.org/10.1016/j.ijfatigue.2018.06.008>.
 47. Wang Q, Ji B, Fu Z, Ye Z. Evaluation of crack propagation and fatigue strength of rib-to-deck welds based on effective notch stress method. *Constr Build Mater.* 2019 Mar 20;201:51–61, <https://doi.org/10.1016/j.conbuildmat.2018.12.015>.
 48. DIN 22261-1. Excavators, spreaders and auxiliary equipment in opencast lignite mines - Part 1: Construction, commissioning and monitoring.